ELSEVIER

Biochimica et Biophysica Acta 1235 (1995) 406–418

BBA Biochimica et Biophysica Acta

Adaptive changes in lipid composition of skeletal sarcoplasmic reticulum membranes associated with aging

Arkadi G. Krainev [a], Deborah A. Ferrington [a], Todd D. Williams [b], Thomas C. Squier [a], Diana J. Bigelow [a,*]

[a] *Department of Biochemistry, University of Kansas, Lawrence, KS 66045-2106, USA*
[b] *Mass Spectrometry Laboratory, University of Kansas, Lawrence, KS 66045-2106, USA*

Received 27 June 1994; revised 21 November 1994; accepted 7 December 1994

Abstract

We have undertaken a detailed examination of changes associated with aging in lipid composition and corresponding physical properties of hindlimb skeletal sarcoplasmic reticulum (SR) membranes isolated from young (5 months), middle-aged (16 months), and old (28 months) Fischer strain 344 rats. Silica gel HPLC chromatography was used to separate phospholipid headgroup species. Subsequent reversed-phase HPLC was used to resolve fatty acid chain compositions of phosphatidylcholine, phosphatidylethanolamine, and phosphatidylinositol species. For all three phospholipid pools, significant age-related variations are observed in the abundance of multiple molecular species, particularly those having polyunsaturated fatty acid chains. Using mass spectrometry (fast atom bombardment and tandem techniques) to distinguish ester- from ether-linked phosphatidylethanolamine species, we demonstrate that overall plasmenylethanolamine content is substantially increased with age, from 48 mol% to 62 mol%. A substantial increase is also observed in the single molecular species 18:0-20:4 phosphatidylinositol suggesting implications for signalling pathways. In addition, associated with senescence we find a significant increase in the rigidifying lipid, cholesterol. Despite these changes in lipid composition of different aged animals, the average bilayer fluidity examined at several bilayer depths with stearic acid spin labels, is not altered. Neither do we find differences in the rotational mobility of maleimide spin-labeled Ca^{2+}-ATPase, as determined from saturation-transfer electron paramagnetic resonance, which is sensitive to both the fluidity of lipids directly associated with the Ca^{2+}-ATPase and to its association with proteins.

Keywords: ATPase, Ca^{2+}-; Sarcoplasmic reticulum; Membrane composition; ST-EPR; Mass spectrometry; Aging

1. Introduction

Glycerophospholipids of biological membranes represent a heterogeneous population of molecular species defined by (a) the chemical structure of the polar headgroup, (b) the type of linkage to the glycerol moiety, and (c) the structure of the aliphatic chains at both *sn*-1 and *sn*-2 positions. Relative proportions of these molecular species in a biological membrane are largely affected by diet, patho-physiological conditions, and age of the organism [1–3]. The composition of biological membranes is an important determinant of both the general physical properties of the bilayer, and the available concentration of specific metabolites for a variety of cellular functions, including pathways related to signal transduction, immune defense, and lipid synthesis and turnover [4]. Fluidity is possibly the most critical physical property of the bilayer with respect to the dynamics and catalytic activity of integral membrane proteins [5].

Dysfunction of one integral membrane protein, the sarcoplasmic reticulum (SR) Ca^{2+}-ATPase, which actively sequesters calcium ions away from relaxing muscle fibers, has been implicated as the source of the longer relaxation

Abbreviations: CID, collisionally-induced dissociation; CL, cardiolipin; EPR, electron paramagnetic resonance; FAB, fast atom bombardment; HPLC, high-performance liquid chromatography; LPC, lysophosphatidylcholine; MB, magic bullet (matrix for mass spectrometry); PA, phosphatidic acid; PC, phosphatidylcholine; PE, phosphatidylethanolamine; PI, phosphatidylinositol; PS, phosphatidylserine; SASL, stearic acid spin label; SPH, sphingomyelin; ST-EPR, saturation transfer electron paramagnetic resonance; SR, sarcoplasmic reticulum; TEA, triethanolamine.

* Corresponding author. Fax: +1 (913) 8645321.

SSDI 0005-2736(94)00317-3

times of skeletal muscle observed in aged individuals [6]. Previous work has shown that efficiency of calcium transport and the functional stability of the Ca^{2+}-ATPase are compromised with age [7,8]. Both characteristics may be explained in terms of changes in SR lipid composition that result in the inability of the membrane-spanning peptides of the Ca^{2+}-ATPase to pack efficiently within the hydrophobic bilayer. For example, in a number of biological membranes, aging is associated with an increase in the content of rigidifying membrane components, such as cholesterol and saturated phospholipid molecules [5,9]. The presence of specific lipids has also been shown to affect the ability of the Ca^{2+}-ATPase to pack efficiently and stably in the SR membrane [10]. However, questions regarding the possible role of SR lipid composition in age-related functional changes cannot be seriously addressed without information, currently lacking, regarding possible age-related changes in SR lipid composition. In addition, direct measurements of their consequences for bilayer structure are needed.

Therefore, we are interested in identifying possible changes in lipid composition of SR membranes associated with aging, and to understand how they may relate to membrane fluidity and function of the Ca^{2+}-ATPase. For the present study, we have used a combination of HPLC and mass spectrometric techniques to identify compositional changes of individual lipid molecular species in SR membranes isolated from skeletal muscle of young adult (5 months), middle-aged (16 months), and old (28 months) Fischer strain 344 rats. In order to understand the structural consequences that multiple changes in a heterogeneous lipid composition may have for the bilayer, we have measured the rotational dynamics of the predominant SR membrane protein, the Ca^{2+}-ATPase, as well as that of the surrounding SR lipids. These measurements have utilized both saturation-transfer and conventional electron paramagnetic resonance (EPR) of nitroxide spin labels. A preliminary presentation of a portion of this work was made at the 37th Annual Meeting of the Biophysical Society [11].

2. Materials and methods

2.1. Materials

HPLC grade solvents were obtained from Fischer (Medford, MA). Choline chloride and synthetic phospholipid standards were obtained from Sigma (St. Louis, MO). Phospholipids from animal sources were obtained from Avanti Polar-Lipids (Alabaster, AL). All other commercial chemicals were of reagent grade.

2.2. Preparation of rat skeletal SR membranes

Native SR vesicles were prepared from rat hindlimb muscles as described previously [12]. Vesicles were suspended in a medium containing 0.3 M sucrose and 20 mM Mops (pH 7.0) and stored at $-70°$ C. For each of three simultaneous preparations, SR membranes were isolated from pooled muscle tissue of two each young (5 months), middle-aged (16 months), and old (28 months) male rats (Fischer strain 344, Harlan Sprague Dawley, Indianapolis, IN).

2.3. Assays of enzymatic activity

ATP hydrolytic activity was assayed under various conditions in order to assess relative proportions of SR, sarcolemmal, transverse tubule, and mitochondrial membrane in the muscle membrane preparation. Calcium-dependent ATPase activity was assayed at 25° C as a marker for SR membranes, by colorimetric determination of inorganic phosphate released from vesicles made leaky to calcium by the addition of 4 μM calcium ionophore A23187 according to Lanzetta et al. [13]. The reaction medium contained 0.05 mg SR protein/ml, 100 mM KCl, 5 mM $MgCl_2$, 4 μM A23187, 25 mM Mops (pH 7.0) and either 0.1 mM $CaCl_2$ or 0.1 mM EGTA. The reaction was started by addition of 5 mM ATP and the initial rate of release of inorganic phosphate was used to calculate activity. Activity assayed in the presence of EGTA (basal activity) was subtracted from that assayed in the presence of $CaCl_2$ (total ATPase activity) in order to obtain calcium-dependent ATPase activity. Vesicular integrity was assessed from the ratio of calcium-dependent ATPase activity in the presence to that in the absence of the calcium ionophore, A23187.

Calcium-independent ATPase (basal) activity was taken as an indication of total contamination by other membranes of the muscle cell. Sarcolemmal membrane content was determined by measuring inhibition of basal ATPase activity by 2 mM ouabain. Mitochondrial membrane content was measured from the inhibition of basal ATPase activity by 16 μg/ml oligomycin. Transverse tubule membrane content was determined from divalent ATPase activity [14]. This assay involved measuring ATPase activity under basal conditions with 1.6 mM $CaCl_2$ and without $MgCl_2$.

2.4. Extraction of SR phospholipids

Lipids of SR membranes were extracted according to Folch et al. [15] as modified by Hidalgo et al. [16]. Lipid extracts were stored at $-20°$ C dissolved in chloroform deoxygenated by bubbling N_2 gas for 30 min. The extent of lipid peroxidation in sample extracts and control solutions of authentic 18:0-20:4 PC standards prepared and stored in the same way was monitored by absorbance at 234 nm characteristic for oxidized polyunsaturated fatty acids [17]. Lipid peroxidation was found to be negligible under the conditions employed. Lipid extracts were assayed for phospholipid phosphorus [18] and cholesterol (using a kit from Abbott, according to Allain et al. [19]).

2.5. HPLC procedures

SR membrane phospholipid classes were separated using high-performance liquid chromatography as described by Blank and Snyder [20] with minor modifications as described below. Lipid extracts were dried under a stream of nitrogen and dissolved in a deoxygenated 2-propanol/hexane/water (54:40:6, v:v) mixture. 0.1 ml of this solution containing up to 1400 nmol of phospholipid phosphorus was injected into the HPLC apparatus, constructed of two sequentially connected Alltech ECONOSPHERE SILICA 5 μm columns (250 mm × I.D. 4.6 mm). The elution rate was 1 ml/min using a complex gradient solvent system maintained with an ISCO 2360 gradient programmer. The eluant was composed of 2-propanol/hexane (1:1, v:v) mixture and 3% to 8% of water with a 5-min exposure to 0.75 mM of lithium chloride (Fig. 1A).

Detection was by absorption at 205 nm. Retention times (R_t) of major phospholipid components were determined using standards of commercially available pure lipids from natural sources. R_t values vary depending on the degree of silica column 'polarization', i.e., the time of contact with strong polar solvent such as water. Periodically, namely after ca. 25 injections, the precolumn filler was changed and the columns were regenerated using SUPELCO silica column regeneration solution. Peaks were collected and subjected to phosphorus analysis as described above. Usually, 92–95% of the total lipid phosphorus injected was recovered after chromatography.

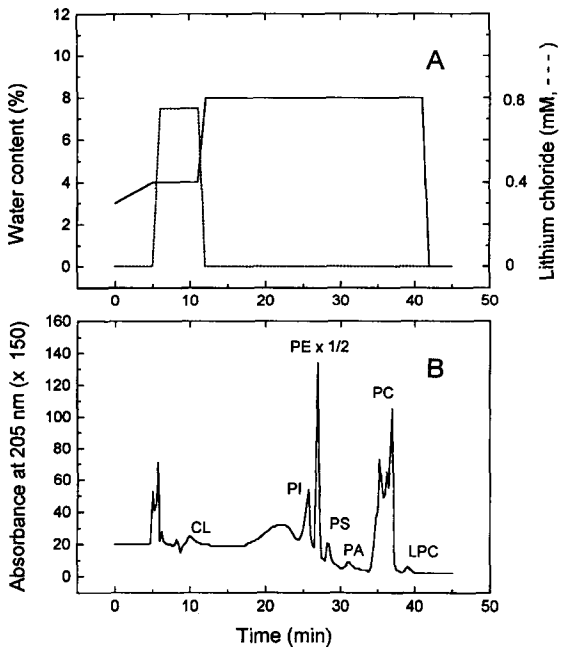

Fig. 1. HPLC separation of phospholipid headgroup species from lipid extracts of skeletal SR membranes from young (5 months) Fischer 344 rats. 189 nmol of lipid phosphorus was injected in an 100 μl volume and eluted using a gradient system (A); the elution profile is shown in (B). Peaks were identified using retention times (R_t) obtained from the following authentic standards: R_t = 9–11 min, heart cardiolipin (CL); R_t = 24–26 min, liver L-α-phosphatidylinositol (PI); R_t = 26–27 min, bovine brain L-α-phosphatidylethanolamine (PE); R_t = 28–30 min, brain L-α-phosphatidylserine (PS); R_t = 31–32 min, 1-palmitolyl-2-oleoyl-*sn*-glycero-3-phosphate (PA); R_t = 34–38 min, bovine brain L-α-phosphatidylcholine (PC); R_t = 39–40 min, L-α-lysophosphatidylcholine (LPC).

Phosphatidylcholine (PC), phosphatidylethanolamine (PE) and phosphatidylinositol (PI) fractions were separated into molecular species on a 4.6 × 250 mm ISCO Spherisorb 5 μm ODS-2 C_{18} reversed phase column essentially as previously described [21]. The elution was performed with a methanol/water/acetonitrile 90.5:7:2.5 (v:v) mixture containing 20 mM choline chloride at a flow rate of 2.0 ml/min. The molecular species of phospholipids in each peak were identified by relative retention times and equivalent chain length procedures reported by Wiley et al. [22]. Fractions collected from the column were dried under a stream of nitrogen and redissolved in 20 μl of the same mixture. Samples of individual fractions were rechromatographed prior to mass spectrometry analysis on silica column as described above, but without LiCl.

Quantitation of individual molecular species' chromatograms was assessed by phospholipid phosphorus analysis as described above and confirmed by integration of peak areas using authentic standards with an appropriate amount of double bonds per molecule. It should be noted however that spectrophotometric detection at 205 nm is incapable of detection and quantitation of lipids with saturated fatty acids at both *sn*-1 and *sn*-2 positions. However, according to previous studies [23,24], these phospholipid species account for only about 1–2% of the total lipid content in animal sources.

2.6. Mass-spectrometry procedures

Selected peaks in PC and PI pools and all fractions in PE pool were subjected to fast atom bombardment (FAB) and tandem mass spectrometry analysis on an AUTOSPEC-Q tandem hybrid mass spectrometer (VG Analytical, Manchester, UK) equipped with an OPUS data system. FAB mass spectrometry experiments were performed using a cesium gun operated at 20 keV energy and 2 μA emission. Triethanolamine (TEA) and magic bullet (MB, dithioerythritol/dithiothreitol, 1:3 (w/w)) were used as matrices. Collisionally induced dissociation (CID) experiments were performed with precursor ions attenuated 50% with xenon in the collision quadruple. The collision energy used was 60 eV (laboratory frame of reference). The analyzer quadruple was tuned to 1.5 atomic weight units full width at half height and the precursor ion was transmitted with MS1 tuned to 1500 resolution. The scan rate was 1 s/100 atomic weight units and 5 scans were integrated. The method used to determine the fatty acid side chains was adapted from observations by Gross et al. [25].

The molecular weight of PCs in collected HPLC peaks was determined using FAB in the positive ion mode with

MB as a matrix. The fatty acid composition of individual PCs was made by collisionally activating the corresponding $(M-15)^-$ ion generated when the same sample was ionized from TEA in negative ion mode. CID yielded abundant $RCOO^-$ ions, providing the molecular weight of attached fatty acids. PE and PI samples were analyzed in negative ion mode exclusively and were always run in two matrices, TEA and MB. Both matrices gave abundant matrix adducts, primarily $(Phospholipid + Matrix\text{-}H)^-$ ions. The use of two matrices simplified the identification of $(M-H)^-$ ions. Fatty acid indicating ions from PE and PI samples were generated by CID of $(M-H)^-$.

2.7. Spin labeling

Hydrocarbon chain mobility was measured with the fatty acid spin label, a *N*-oxyl-4′,4′-dimethyloxazolidine derivatives of stearic acid (Aldrich), designated 5-, 7-, 10-, 12-, and 16-SASL (stearic acid spin label) using conventional EPR techniques. The spin label was diluted from a stock solution in dimethylformamide into ethanol before adding to SR at a ratio of less than one spin label/200 phospholipids, with the final ethanol concentration less than 1%. To measure rotational motion of the Ca^{2+}-ATPase protein, SR was labeled with a short chain maleimide spin label, *N*-(1-oxyl-2,2,6,6-tetramethyl-4-piperidinyl)maleimide (Aldrich) as described previously [26,27].

2.8. EPR spectroscopy

EPR spectra were obtained with a Varian E-109 spectrometer. Submicrosecond rotational motion of spin labels was detected by conventional EPR (first harmonic absorption in-phase, designated V_1) using 100-kHz field modulation (with peak-to-peak amplitude of 2 G) and a microwave field intensity of 0.032 G. Submillisecond rotational motion was detected by saturation-transfer EPR (second harmonic absorption out-of-phase, designated V_2') using 50-kHz field modulation (with a modulation amplitude of 5 G) and a microwave field intensity of 0.25 G. All EPR samples were suspended in 0.3 M sucrose, and 20 mM Mops (pH 7.0).

2.9. Spectral analysis

Conventional EPR spectra of fatty acid spin labels were evaluated by measuring the effective order parameter *S*, which depends only on the angular amplitude of the motion of the probe. Assuming very fast anisotropic motion of the probe ($\tau_r < 1$ ns; where τ_r is the effective rotational correlation time), an increase in rate has no effect on the positions of the spectral extrema. Values of *S* greater than 0.3 can be measured using the standard formula relating *S* to both inner and outer extrema [28,29], i.e., $S = 1.66 \cdot ((T_\parallel' - (T_\perp' + C))/(T_\parallel' - 2(T_\perp' + C)))$, where $C = 1.4 - 0.053 \cdot (T_\parallel' - T_\perp')$. $2T_\perp$ and $2T_\parallel'$ are the measured inner and outer extrema resolved in the EPR spectrum in gauss.

The effective rotational correlation times for maleimide spin-labeled SR were determined from ST-EPR spectra using a plot of lineshapes versus correlation time based on reference spectra of known correlation time obtained from isotropically tumbling spin-labeled hemoglobin in aqueous glycerol solutions [30].

3. Results

3.1. Characterization of SR preparations

Native SR membranes were purified from pooled skeletal muscle of (two animals each) young adult (5 month), middle age (18 month) and old (28 month) Fischer 344 rats. This purification results in substantial enrichment of the SR membrane, but not without some co-purification of other organellar membranes that are in close proximity within the muscle cell. The extent of this contamination by other muscle membranes presents considerable variability between preparations. Thus for this study we have compared different SR samples within the same preparation in order to eliminate differences due to prep-to-prep variation. Approximately 12% of the total ATP hydrolysis activity of these preparations arises from calcium-independent ATPases (Table 1). These ATPases are associated with mitochondrial, sarcolemmal, and transverse tubule membranes. Since their lipid compositions are quite distinct from that of SR, it is important to take into consideration possible contributions from their component lipids in our analysis. We have therefore quantitated the relative contributions of these membranes in our SR preparations by utilizing specific inhibitors of: (1) the F_1-F_o-ATPase in

Table 1
Relative proportions (%) of marker membrane activities [a]

Marker enzymes	5 months	16 months	28 months
Basal ATPase [b]	11.8 ± 0.3	11.3 ± 0.3	12.1 ± 1.1
Sarcolemmal ATPase [c]	N.D. [d]	N.D. [d]	1.2 ± 0.1
Mitochondrial ATPase [e]	4.9 ± 0.6	5.3 ± 0.2	4.7 ± 0.2 *
Transverse-tubule ATPase [f]	6.7 ± 0.3 **	4.8 ± 0.1	5.8 ± 0.9

[a] All activities are expressed as percent of total (+Ca)-ATPase activity. Total (+Ca)-ATPase activity is independent of age and equals to 4.1 ± 0.3 I.U. Data are means of duplicate trials ± S.D.
[b] Basal (calcium-independent) ATPase activity was assayed with EGTA present instead of $CaCl_2$.
[c] ATPase activities inhibitable by addition of 2 mM ouabain.
[d] N.D., not detected.
[e] ATPase activities inhibitable by addition of 16 μg/ml oligomycin. * 28 month sample was significantly different from 16 month sample, at the $P < 0.1$ level.
[f] Transverse-tubule Mg^{2+}-ATPase activities are determined using the reaction conditions as for *a*, with 1.6 mM $CaCl_2$ and without $MgCl_2$. ** 5 month sample was significantly different from 16 month sample, at the $P < 0.05$ level.

Table 2
Cholesterol content and protein/phospholipid ratio in rat skeletal SR preparations [a]

Age	Cholesterol (μg/μmol lipid phosphorus)	Protein/lipid ratio (mg/μmol lipid phosphorus)
5 months	33.1 ± 0.7	1.8 ± 0.2
16 months	32.4 ± 1.2	2.3 ± 0.2
28 months	36.3 ± 0.3 *	2.4 ± 0.3

[a] Data are mean values of three separate determinations ± S.E.
* 28 month sample was significantly different from 16 month and 5 month samples, at the $P < 0.05$ level for both.

mitochondrial membranes, i.e., oligomycin, and (2) the Na^+/K^+-ATPase of the sarcolemma, i.e., ouabain, as well as assaying the activity of (3) the ATPase of transverse tubular membranes. We find that mitochondrial and transverse tubule membrane ATPases contribute roughly equal specific activities to the total basal activity; sarcolemmal membranes are virtually absent from these preparations (Table 1). Age-related variations in relative membrane composition are minimal. However, small but statistically significant decreases in mitochondrial contamination ($P < 0.1$) are observed at 28 month and in transverse tubules at 16 month ($P < 0.05$). Nevertheless, the content of SR membranes is unchanged with age of animals.

Lipid extracts from each preparation were subjected to total cholesterol and lipid phosphorus analysis; SR membranes were subjected to lipid phosphorus and protein analysis. The results are summarized in Table 2. We find no significant age-related changes in protein/lipid ratios; however, old animals exhibit a 10–12% increase in cholesterol content compared with young and middle-aged animals. This result agrees with other studies in this laboratory comparing cholesterol content of 5 month with 28 month rat skeletal SR in which we consistently have observed increased cholesterol (17 ± 6%, $n = 6$) in senescent animals.

3.2. Separation of phospholipid headgroup classes

Fig. 1 shows a normal-phase HPLC chromatogram of a total lipid extract of rat skeletal SR membranes. Each eluted peak was identified by comparison to retention times of authentic standards prepared from commercially available pure lipids. Identification of selected PC, PE and PI fractions was confirmed by mass spectrometry. All major phospholipid classes for all three preparations were resolved with one exception; resolution of PA was not achieved for middle-aged animals (Table 3). It should be noted, however, that sphingomyelin was not detected under the conditions employed. In these membranes, lysophosphatidylcholine (LPC) was detected in amounts of 0.1–0.2% of total phospholipid phosphorus, indicating that lipid degradation was minimal.

We find the most notable change in the headgroup composition of phospholipid species is the increased cardiolipin level, that is observed in senescence, i.e., between 16 and 28 months (Table 3). Although the increase in this species is small, less than 0.16 mol%, this represents almost a 50% increase with respect to levels in young and middle-aged animals (Table 3). Cardiolipin is a significant and unique component of mitochondrial membranes; the low levels found in SR membrane preparations are generally thought to arise from mitochondrial contamination. Therefore, the observed increases in cardiolipin abundance may reflect age-related changes of this species in mitochondrial membranes. Small increases and decreases in PE and PS, respectively, are observed between 5 and 16 months (Table 3).

3.3. Separation of phospholipids into fatty acyl chain species

HPLC peaks corresponding to major phospholipid head group species, PC and PE, and PI, were each rechromatographed on a C_{18} reversed-phase column (Fig. 2). Under these conditions phospholipid elution is influenced by both chain length and degree of unsaturation. In most cases the resulting peaks correspond to individual molecular species of PC, PE and PI (Tables 4–6). Comparison of HPLC traces associated with SR lipid extracts from young, intermediate and old animals allows a reliable detection of age-related changes in phospholipid composition of SR membranes.

We used mass spectrometry to confirm retention time-based assignment of molecular species of PE, the major plasmalogen-containing species in SR membranes. Exact acyl carbon chain length and double bonds in each acyl group cannot be deduced from the FAB-produced ion alone. For example, $(M\text{-}H)^-$ ion mass of 747 can corre-

Table 3
Lipid composition (mol%) of skeletal SR membranes [a]

Age	CL [b,c]	PI	PE [b]	PS [b]	PA	PC
5 months	0.37 ± 0.05 #	7.6 ± 1.0	17.9 ± 0.5	4.1 ± 0.1	1.3 ± 0.1	68.7 ± 0.2
16 months	0.30 ± 0.01 **	8.0 ± 0.5	20.2 ± 0.6 **	3.2 ± 0.1 **	- [d]	68.4 ± 0.6
28 months	0.46 ± 0.01 #	7.9 ± 0.2	21.0 ± 0.6 **	3.1 ± 0.4 *	1.4 ± 0.1	66.2 ± 0.6

[a] Abbreviations used are the same as in Fig. 1. Data are mean values of three or four separate determinations ± S.E.
[b] Lipid species exhibiting significant age-related changes: * $P < 0.05$ and ** $P < 0.01$ from the values of 5 month animals.
[c] Lipid species exhibiting significant age-related changes # $P < 0.01$ from the values of 16 month animals.
[d] PA was not separated from PC in these experimental series.

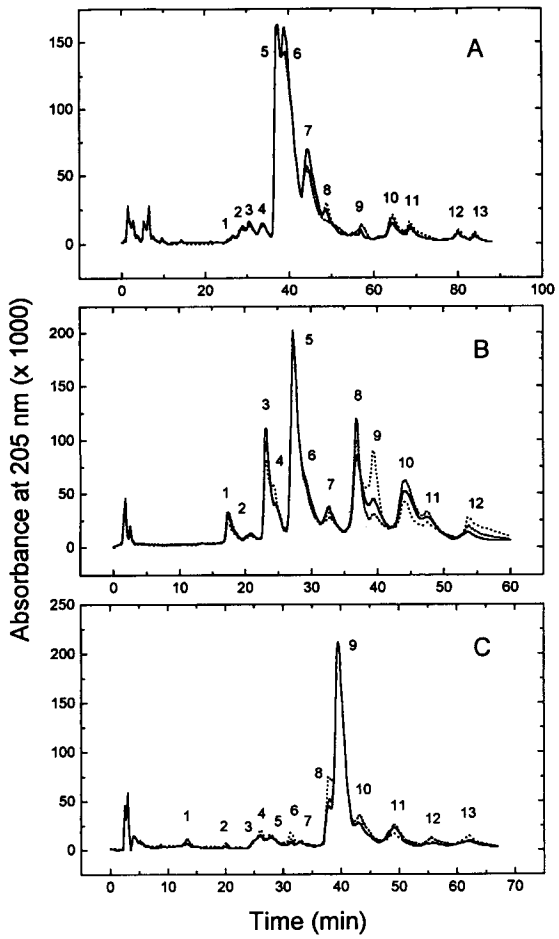

Fig. 2. C_{18} reversed-phase HPLC separation of the molecular species of skeletal SR lipids: PC (A), PE (B), and PI (C). SR lipids were isolated from 5 months (dotted lines), 16 months (dashed lines), and 28 months (solid lines) old animals. Peaks are numbered; identification and quantitation of corresponding species are shown in Tables 4–6. Identification of peaks by relative retention times and mass spectrometry is described in detail in Materials and methods. To ease comparison, all HPLC chromatograms are normalized to the height of the highest peak in preparations from old animals.

spond to either 16:0-22:6 acetenyl-acyl PE, 18:0-18:0 diacyl or 16:0-20:0 diacyl PE. Therefore, we employed tandem mass spectrometry CID analysis to distinguish ether-linked from ester-linked acyl chains at the *sn*-1 position of the glycerol moiety [31]. Authentic PE standards of known chemical structure were examined by CID of $(M\text{-}H)^-$ ions. As little as 10 pmol of PE with ester-linked acyl chains applied to the FAB probe provided abundant $RCOO^-$ ions. However, application of ether linkage-containing PEs failed to provide a diagnostic ion for the ether-linked chain length. PEs with mixed ether and ester linkages gave abundant ions for only the ester linked chain. Thus, ether-linked acyl chains were assigned to PE samples from SR membranes on the basis of a lack of signal between 200 and 400 atomic weight units in the CID spectrum of $(M\text{-}H)^-$ ions required to account for the complete molecular weight of the PE. Fig. 3A and B is an example of PEs with a 18:2-22:6 di-acyl- and 16:0-22:5 acethenyl-acyl-composition, respectively. Only the carboxylated ions are detected in CID spectra.

Resolution of plasmenyl ethanolamines in lipid fractions from different aged animals demonstrates significant age-related changes in several plasmenyl species, particularly 18:0-22:6 and 16:0-20:4 acetenyl-acyl-phosphatidyl-ethanolamines (Table 5). Overall, ethanolamine plasmalogen containing peaks increased with age from 48 to 62 mol%; most of this change had occurred by middle age.

Thus, we find that the molecular species composition observed here (Tables 4–6) is similar to that reported for skeletal SR membranes of other animals [32,33]. The present results indicate multiple age-related variations in the abundance of certain individual species in PC, PE and PI fractions. The most dramatic changes involve those species containing polyunsaturated fatty acyl chains; some decrease with age; others correspondingly increase (Tables 4–6). For each headgroup pool (PC, PE and PI) the average level of unsaturation, indicated by the mean number of carbon-carbon double bonds per phospholipid molecule, shows only modest changes with age. We note that no new molecular species appear in SR membranes of different-aged animals.

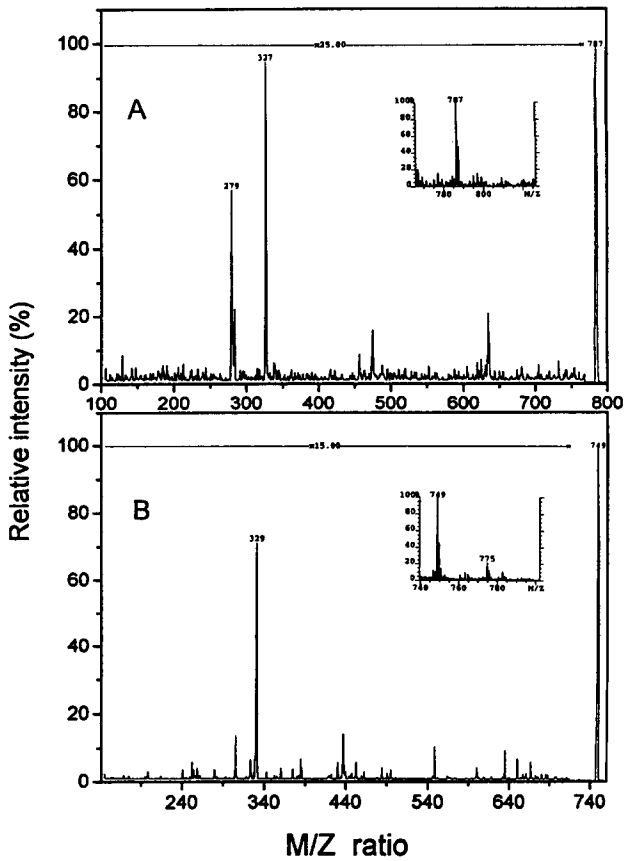

Fig. 3. CID mass-spectra of 787 (A) and 749 (B) ions derived from FAB^- ionization (insets) of PE samples collected from HPLC separation (Fig. 2B), peaks 1 and 7, respectively. Details are described in the text.

Table 4
Molecular species of rat skeletal SR PC [a]

Peak No.	Molecular species [b]	5 months	16 months	28 months
1	16:1-20:4	trace	trace	trace
2	16:0-20:5	1.1 ± 0.1	0.7 ± 0.1	1.1 ± 0.1
3	18:2-20:4	2.1 ± 0.2	1.8 ± 0.1	1.8 ± 0.2
4	16:0-16:1 [c]	2.6 ± 0.2	2.6 ± 0.2	2.4 ± 0.2
5 [d]	16:0-22:6($n-3$)	14.1 ± 1.2 *	16.0 ± 0.7 *	10.0 ± 0.6
6 [d]	16:1-18:1 + 16:0-20:4 + 16:0-18:2	33.0 ± 1.3 *	33.2 ± 0.3 *	37.5 ± 0.8
7	18:1-18:2	23.0 ± 2.1	24.6 ± 2.0	25.2 ± 2.1
8 [d]	16:0-20:4 AA	8.9 ± 0.5 *	6.5 ± 0.4 *	10.6 ± 0.4
9	16:0-18:1 [c]	1.1 ± 0.1	2.2 ± 0.3	1.2 ± 0.1
10	18:0-20:4	4.7 ± 0.4	4.6 ± 0.8	3.1 ± 0.3
11 [e]	18:0-18:2	9.4 ± 0.8	7.7 ± 0.7 #	7.2 ± 0.6 ##
12	18:0-20:4 AA	trace	trace	trace
13	18:0-22:5	trace	trace	trace
Mean unsaturation [f]		3.5	3.5	3.4

[a] PC molecular species were separated by reversed-phase (C_{18}) HPLC, peak numbers correspond to those shown in Fig. 2A. Quantitation was assessed as described in Materials and methods. Values are expressed in mol%.
[b] Tentative assignment based on relative retention times. AA indicates acethenyl-acyl-phosphatidylcholines.
[c] Assignment was confirmed by mass spectrometry.
[d] Major molecular species (≥ 5 mol%) exhibiting significant age-related changes from the values of 28 month animals (* $P < 0.01$).
[e] Major molecular species (≥ 5 mol%) exhibiting significant age-related changes from the values of 5 month animals (# $P < 0.1$ and ## $P < 0.05$).
[f] Calculated mean number of carbon-carbon double bonds per phospholipid molecule.

In contrast to PC and PE fractions, the 18:0-20:4 species is the predominant species of PI, comprising more than 50 mol% of these phospholipids. A substantial increase is observed in this fraction from young to old age, at the expense of a number of other molecular species having unsaturated chains, for example, 18:0-22:6, 18:1-20:3 and 16:0-22:5 (Table 6). Although the statistical variation of the 18:0-20:4 species at middle age does not allow us to define the age-related progression of this change, statistically significant trends in these other species indicate a compositional remodelling that occurs throughout the animal's lifespan with the greatest extent of these changes occurring by middle age.

3.4. Spin-label EPR measurements of protein and lipid dynamics

Changes in lipid composition may influence bilayer physical properties, which have been shown to directly modulate the transport activity of a large number of trans-

Table 5
Molecular species of rat skeletal SR PE [a]

Peak No.	Molecular species [b]	5 months	16 months	28 months
1	18:2-22:6 *di*	0.9 ± 0.1	1.5 ± 0.5	1.2 ± 0.1
2	16:1-22:5 *di*	1.9 ± 0.3	0.7 ± 0.3	2.2 ± 0.3
3 [c]	16:0-22:6 *di*	7.5 ± 1.8	10.3 ± 0.2 *	9.3 ± 0.4
4 [c]	16:1-22:4 *di* + 16:0-20:4 *di*	9.6 ± 0.4	5.1 ± 0.7 ***	5.9 ± 0.6 ***
5 [c]	16:0-22:6 AA + 18:1-18:2 *di*	17.9 ± 2.8	23.4 ± 1.4 **	22.2 ± 1.3 *
6 [d]	16:0-20:4 AA	6.6 ± 2.8 #	5.1 ± 0.7 ##	11.6 ± 1.1
7	16:0-22:5 AA	5.7 ± 2.6	4.4 ± 0.9	7.0 ± 0.3
8 [d]	18:0-22:6 *di*	16.0 ± 2.9	20.4 ± 0.4 ##	13.9 ± 1.4
9 [c]	18:0-20:4 *di* + 18:0-18:2 *di*	16.0 ± 0.9	2.9 ± 1.4 ***	5.9 ± 0.5 ***
10 [c]	18:0-22:6 AA	13.2 ± 0.9	17.5 ± 0.3 ***	14.0 ± 1.6
11	18:0-22:5 *di* + 18:0-18:2 AA	1.9 ± 0.1	7.3 ± 0.2	5.8 ± 0.1
12	18:0-22:5 AA	2.8 ± 0.3	1.4 ± 0.1	1.2 ± 0.1
Plasmalogenic species [c,e]		48.1 ± 4.8	59.1 ± 1.9 **	61.8 ± 2.4 **
Mean unsaturation [f]		4.6	5.1	5.1

[a] PE molecular species were separated by reversed-phase (C_{18}) HPLC, peak numbers correspond to those shown in Fig. 2B. Quantitation was assessed as described in Materials and methods. Values are expressed in mol%.
[b] Assignment based on mass-spectrometry data; *di* stands for di-acyl-phosphatidylethanolamines; AA stands for acethenyl-acyl-phosphatidylethanolamines.
[c] Major molecular species (≥ 5 mol%) exhibiting significant age-related changes from the values of 5 month animals (* $P < 0.1$, ** $P < 0.05$ and *** $P < 0.01$).
[d] Major molecular species (≥ 5 mol%) exhibiting significant age-related changes from the values of 28 month animals (# $P < 0.05$ and ## $P < 0.01$).
[e] Percentage of lipid phosphorus found in plasmalogen-containing peaks.
[f] Calculated mean number of carbon-carbon double bonds per phospholipid molecule.

Table 6
Molecular species of rat skeletal SR PI [a]

Peak No.	Molecular species [b]	5 months	16 months	28 months
1	14:0-22:6	trace	trace	trace
2	16:0-16:1	trace	trace	trace
3	16:0-18:2	trace	trace	trace
4 [c]	16:0-22:5($n-3$)	5.5±0.5	3.6±0.4 **	3.0±0.4 **
5	18:1-18:2	4.5±0.2	4.0±0.2	3.4±0.2
6 [c,d]	18:1-20:3($n-3$)	7.1±1.0	3.2±0.7 **,#	2.2±0.3 **
7	16:0-20:3($n-3$)	trace	trace	trace
8 [c]	18:0-22:6	5.8±0.9	3.6±0.8 *	2.8±0.5 **
9 [c]	18:0-20:4 [e]	50.5±3.3	54.7±5.9	62.1±3.6 *
10 [d]	18:0-18:2 [e]	13.7±5.2	15.6±1.5 #	13.3±0.3
11 [c]	18:1-18:1	5.2±0.5	7.8±1.0 *	7.1±0.6 *
12	18:0-20:3($n-6$)	3.1±0.6	3.5±0.6	2.8±0.5
13	18:0-18:1 [e]	4.7±0.5	3.9±0.4	3.3±0.5
Mean unsaturation [f]		3.6	3.4	3.5

[a] PI molecular species were separated by reversed-phase (C_{18}) HPLC, peak numbers correspond to those shown in Fig. 2C. Quantitation was assessed as described in Materials and methods. Values are expressed in mol%.
[b] Tentative assignment based on relative retention times.
[c] Major molecular species (≥ 5 mol%) exhibiting significant age-related changes from the values of 5 month animals (* $P < 0.05$ and ** $P < 0.01$).
[d] Major molecular species (≥ 5 mol%) exhibiting significant age-related changes from the values of 28 month animals (# $P < 0.1$).
[e] Assignment was confirmed by mass spectrometry.
[f] Calculated mean number of carbon-carbon double bonds per phospholipid molecule.

port proteins, including the Ca^{2+}-ATPase [34,35]. The transport activity of the Ca^{2+}-ATPase from skeletal SR has been shown to be modulated by the surrounding lipid dynamics [27,36], or through changes in protein-protein associations [37,38]. Therefore, the measurement of the rotational dynamics of both the lipid and Ca^{2+}-ATPase in SR membranes from young, intermediate, and aged animals is critical to an assessment of how the multiple age-related changes in membrane lipid composition may influence the bilayer's physical properties.

Using stearic acid spin labels (SASL) with a nitroxide reporter group covalently linked to different positions along the hydrocarbon acyl chain relative to the α-carbonyl group, we were able to assess any possible changes in the dynamic properties of the bilayer associated with aging. Since spin-label EPR measurements resolve bulk lipids that are relatively unperturbed by the Ca^{2+}-ATPase from those lipids adjacent to the Ca^{2+}-ATPase [39], we were able to assess changes in the physical properties of both the bulk and protein-associated lipid environments. Those lipids in direct contact with the Ca^{2+}-ATPase represent about 40% of the total membrane lipids in skeletal SR, and are readily resolved [36]. There were no changes in the rotational dynamics of either population of lipids associated with aging, as assessed by spectral subtractions which indicate no spectral changes (data not shown). The apparent order parameters (S) obtained using 5-, 7-, 10-, 12-, and 16-SASL are shown (Fig. 4). All SR membranes exhibit normal fluidity gradients with respect to acyl chain dynamics, i.e., spin probes at the center of the bilayer exhibit less order than those near the bilayer surface [40,41]. Regardless of the position of the nitroxide on the SASL, fatty acyl chain dynamics show no age-related differences.

3.5. ST-EPR measurements of protein rotational diffusion

Measurements of protein rotational diffusion provide a sensitive complementary measurement regarding membrane structure, since rotational diffusion is sensitive to both the membrane viscosity (i.e., acyl chain dynamics) and the extent of protein-protein associations [42,43]. Previous studies regarding age-related effects in SR membranes have suggested that aging is associated with an increased tendency for the Ca^{2+}-ATPase to undergo self-association when subjected to mild heating (37° C) [8]. Therefore, we have utilized conventional- and saturation-transfer EPR (ST-EPR) to measure the rotational dynamics associated with the Ca^{2+}-ATPase (Fig. 5). Conventional EPR (Fig. 5a) is sensitive to nanosecond rotational dynamics related to probe mobility. Utilizing labeling conditions described in detail elsewhere [26,27], a covalent maleimide spin label is covalently attached to the Ca^{2+}-ATPase. Under these labeling conditions approx. 5 nmol of spin label per mg SR (about 0.8 mol MSL/mol Ca^{2+}-ATPase) is rigidly bound to the ATPase as evidenced by the relatively small population of weakly immobilized spin labels (i.e., those probes undergoing nanosecond rotational motion are indicated by W in Fig. 5a and represent about 3–4% of the covalently bound spin labels) relative to those spin-labels that indicate no nanosecond rotational motion

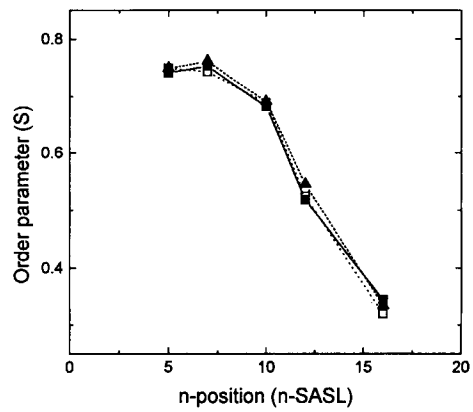

Fig. 4. Order parameters (S) calculated from conventional EPR spectra of a series of n-SASL incorporated into skeletal SR membranes of young (□), intermediate (△), and old (○) rats. Standard errors in S values vary from ±0.005 for young to ±0.006 for old animals. Decreasing order parameters at greater depths in the bilayer are indicative of the fluidity gradient normally observed in lipid bilayers. Spectra were obtained at 4° C using 10 mg SR protein/ml, and a microwave power of 10 mW.

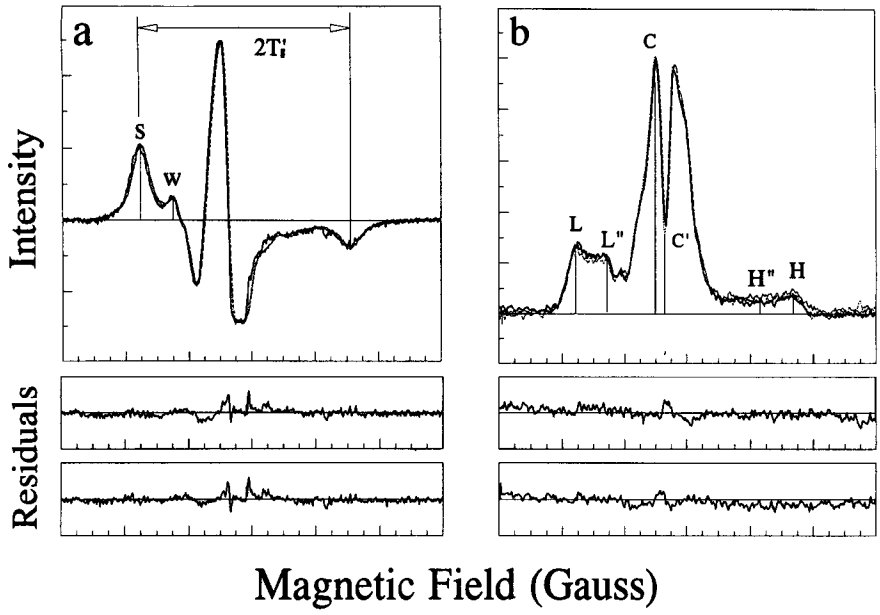

Fig. 5. Spin-label EPR spectra of the Ca^{2+}-ATPase. Top panels: conventional EPR (a) and ST-EPR (b) spectra correspond to maleimide spin labeled Ca^{2+}-ATPase in sarcoplasmic reticulum membranes from young (solid line), intermediate (dashed line), and old (dotted line) animals. Bottom: residuals are shown resulting from subtracting the spectra obtained for the spin-labeled Ca^{2+}-ATPase in old (middle panels) and intermediate (bottom panels) aged animals from the spectra obtained for that from young animals. All spectra were measured at 4° C in 0.3 M sucrose, 20 mM Mops (pH 7.0) at a protein concentration of 70 mg/ml. 1.6 nmol MSL was incorporated per mg of SR, irrespective of the source of the sarcoplasmic reticulum membrane. In all cases the scan width is 120 Gauss. Microwave field intensities used to measure the conventional and ST-EPR spectra were 0.12 and 0.25 Gauss, respectively. Modulation amplitudes used to measure the conventional and ST-EPR spectra were 2.0 and 5.0 Gauss, respectively. The gain used to measure the ST-EPR spectra was approx. 10-fold higher than that used to measure the conventional EPR spectrum. Conventional EPR spectra were analyzed by the outer hyperfine splittings ($2T'_{\|}$) and by the ratio of the low field peaks designated W and S. Correlation times were calculated from ST-EPR line shapes, i.e., from low field peaks L″ and L, center field regions C′ and C, and high field regions H″ and H.

(i.e., S in Fig. 5a). The attachment of spin labels that are immobilized on the conventional EPR time-scale permits the measurement of the hydrodynamic properties of the Ca^{2+}-ATPase using ST-EPR (Fig. 5b).

The shape and intensity of the ST-EPR spectra are sensitive to motion. In particular, rotational diffusion serves as a relaxation mechanism and selectively reduces spectral intensity in diagnostic regions of the spectra (i.e., L″, C′, and H″). We have measured the rotational dynamics of the Ca^{2+}-ATPase from skeletal SR membranes purified from young, intermediate, and aged rat hind-limb skeletal muscle (Fig. 5b). We observe no age-related changes in the shape or intensity of the spectra associated with the rotational dynamics of the Ca^{2+}-ATPase in SR membranes, as evidenced by the negligible intensity associated with the residuals obtained upon spectral subtraction of the ST-EPR spectra associated with membranes obtained from intermediate or aged animals relative to the ST-EPR spectra associated with membranes obtained from young animals. Utilizing reference spectra obtained from spin-labeled hemoglobin we were able to estimate the effective rotational correlation times of the Ca^{2+}-ATPase using both the

Table 7
Spectral parameters from conventional and ST-EPR spectra

Sample	EPR parameters [a]		ST-EPR parameters [b]			
	W/S	$2T'_{\|}$	L″/L	C′/C	H″/H	L″/L_{pp}
5 months (τ_r, μs)	0.24	66.8	0.83 (66 μs)	0.35 (20 μs)	0.70 (107 μs)	0.124 (30 μs)
16 months (τ_r, μs)	0.29	67.0	0.85 (72 μs)	0.35 (20 μs)	0.74 (120 μs)	0.127 (31 μs)
28 months (τ_r, μs)	0.28	66.8	0.81 (61 μs)	0.31 (17 μs)	0.70 (107 μs)	0.119 (28 μs)

[a] Conventional EPR parameters are described by the outer hyperfine splittings ($2T'_{\|}$) and by the W/S ratio, where W and S are the heights of the low field peaks (weakly and strongly immobilized probes, respectively. See Fig. 5A).

[b] ST-EPR line shape and intensity parameters (see Fig. 5B for designations) were used to calculate effective rotational correlation times using an empirical calibration curve obtained from isotropic reference spectra of MSL-Hb in solutions with varying glycerol concentrations. The calibration curves obtained were virtually identical to those previously published [26,30]. The standard deviations of these measurements were 0.03 (L″/L), 0.06 (C′/C), 0.08 (H″/H), and 0.008 (L″/L_{pp}), corresponding to standard deviations in the correlation times of 7 μs (L″/L), 5 μs (C′/C), 23 μs (H″/H), and 5 μs (L″/L_{pp}), respectively.

lineshape and intensity parameters obtained from the spectra (Table 7). These measurements provide increased precision in the measurement of the rotational diffusion of the Ca^{2+}-ATPase, as a result of their different sensitivities to common errors associated with the measurement of ST-EPR spectra [30]. We observe no changes in the effective rotational correlation times obtained from either the lineshape or intensity parameters, again emphasizing that there are no age-related differences in protein-protein associations in SR membranes. The apparent discrepancies between the effective rotational correlation times obtained from the different spectral parameters is indicative of anisotropic rotational motion, as would be expected for a membrane protein undergoing uniaxial rotational motion. These measurements of the rotational dynamics of the Ca^{2+}-ATPase are consistent with earlier measurements of the rotational diffusion of the Ca^{2+}-ATPase from rabbit skeletal SR membranes [26].

4. Discussion

4.1. Summary of results

We have undertaken a detailed examination of SR lipid composition, correlated with direct measurements of dynamic bilayer structure in order to understand environmental influences of lipids on the maintenance of normal calcium regulation by the Ca^{2+}-ATPase in aged skeletal muscle. We have investigated differences in protein/lipid ratios, cholesterol content, phospholipid headgroup composition, and individual fatty acyl chain species of the major headgroup species: phosphatidylcholine (PC) and phosphatidylethanolamine (PE) as well as phosphatidylinositol (PI) in SR membranes. The results of this work indicate that the major phospholipid molecules are 16:1-18:1 and 16:0-20:4 (18:2); 16:0-22:6 and 18:1-18:2; and 18:0-20:4; for PC, PE, and PI, respectively, an observation that highlights the unsaturated character of SR membranes (Tables 4–6). No new phospholipid species appear in SR membranes of different aged animals, although we find substantial variations in the content of cholesterol, plasmalogens, multiple molecular species that contain highly unsaturated fatty acids, and the single molecular species, 18:0-20:4 PI. Despite differences found in the relative abundance of multiple unsaturated phospholipid species and in cholesterol content of SR membranes isolated from different aged animals, the rotational dynamics of spin labels attached to either fatty acids or the Ca^{2+}-ATPase in the SR membrane are unaltered (Figs. 4 and 5). Therefore, even substantial age-related changes in individual lipid species that would be expected to alter bilayer fluidity are associated with compensatory changes in one or more other lipid species. As a consequence, optimal fluidity and hence, optimal enzymatic activity of the major intrinsic SR protein, the Ca^{2+}-ATPase are maintained.

4.2. Rationale for experimental approaches

The aim of this research has been to examine changes which occur in the organism exclusively due to aging rather than diet, disease or environmental conditions. Therefore, as a mammalian aging model, we have utilized the Fischer strain 344 rats, whose genetics and mortality are well characterized. These animals are raised under carefully controlled environmental conditions (see, for review, [44]). We have used three separate age groups of adult (male) animals: (i) 5 months old sexually mature 'young' rats; (ii) 16 months old 'middle-aged' rats; and (iii) 28 months 'old' rats, whose age corresponds to midway through a steep decline in mortality for this rat population. Thus, we have the means to distinguish changes that are associated solely with senescence from those that may be part of a progressive pathway throughout the life span of the individual, or alternatively, associated with late maturation from young adulthood to middle-age.

Recent advances in applications of HPLC techniques have allowed us to separate and identify individual phospholipid species, comparing SR membranes isolated from animals of different ages, without the necessity of chemical derivatization and hydrolytic digestion of phospholipids, and the resulting increased sample variability. We have used a simple two-step resolution of SR lipids, first separating classes that correspond to different headgroups, followed by separation of phospholipids having different fatty acyl chains. This has involved sequential separation on silica and C_{18} reversed-phase HPLC columns, an approach that both facilitates analysis and maintains intact polyunsaturated fatty acids throughout the analytical procedure [22].

4.3. Interpretation of results

In most cases, we expect that observed changes in lipid content of the isolated membranes represent age-related changes associated with the SR. However, it is important to consider the alternate possibility, i.e., that these changes are primarily a result of age-related variations in co-purified mitochondrial and/or transverse tubule membranes. The low abundance of these co-purified membranes in our native SR preparation suggests that this alternative is unlikely (Table 1). Taking into account lipid/protein ratios, specific catalytic activities and relative abundance of marker enzymes for SR [33], transverse tubule [45] and mitochondrial membranes [46,47], an estimated 7 wt% and 11 wt% change in the abundance of an individual molecular species in a contaminating transverse tubule and mitochondrial membranes, respectively, would be required in order to account for even a 1 wt% change in the overall composition of that species in the isolated membranes. Thus with the exception of the small increase in cardiolipin (Table 3), probably arising from mitochondrial membranes, we can assume that observed changes in

membrane composition are primarily due to alterations in SR phospholipid species. Moreover, we can correlate total membrane lipid composition with fluidity measured with fatty acid spin probes since these nondiscriminately sample all composite membranes. On the other hand, our measurements of Ca^{2+}-ATPase protein rotational motion are specific to the SR membrane.

4.4. Effects on bilayer fluidity

Among significant age-related changes in lipid composition, we find that cholesterol content is higher in SR lipid extracts from old animals in comparison with those from young and middle-aged rats (Table 2), and thus represents a change associated only with senescence. This finding is consistent with reports of age-related accumulations of cholesterol in endoplasmic reticulum membranes from several different tissues [48], and predicts a rigidifying effect on the membrane.

The distribution of phospholipid headgroups does not show significant changes associated with aging (Table 3). However, multiple fatty acyl chain species, particularly those with highly unsaturated chains, exhibit both increases and decreases in their relative abundance in the three headgroup classes (PC, PE, and PI) that we examined (Tables 4–6). Estimates of average unsaturation per phospholipid molecule for the three phospholipid pools, that we have assayed, show only modest age-related differences. The limited ability to predict a general physical property such as bilayer fluidity from even a detailed knowledge of membrane composition has motivated our direct measurements of bilayer fluidity using spin label EPR. Previous studies have demonstrated under a variety of experimental conditions that there is a consistent correlation, indeed requirement, of protein rotational mobility for optimal transport function of the SR Ca^{2+}-ATPase [27,36,37,49]. Rotational diffusion of a membrane protein is sensitive to both the fluidity of the surrounding bilayer and the size and shape of the protein [42]. Therefore our complementary measurements using fatty acid spin labels and maleimide spin-labeled Ca^{2+}-ATPase indicate that neither bilayer fluidity nor associations between individual Ca^{2+}-ATPase molecules are altered upon aging (Figs. 4 and 5). Neither are dynamics of the first shell of lipids around the Ca^{2+}-ATPase changed, suggesting that lipid density and lipid packing around the enzyme is unaltered. Therefore, any age-related dysfunction of the Ca^{2+}-ATPase is more likely to be a result of protein modification rather than its lipid environment.

This is in accordance with earlier observations from this laboratory [8], when maleimide spin-labeled Ca^{2+}-ATPase mobility and fatty acid spin probe dynamics were the same in SR membranes from young and old rats, but decreased more rapidly in vesicles from old animals upon heating at 37° C. Thus age-related modification do not involve aggregation per se of the Ca^{2+}-ATPase, but rather a greater tendency for aggregation when subjected to a mild heat stress.

4.5. Other lipid compositional changes

As a result of this study, we have observed several interesting lipid compositional changes that may have more significant consequences for cellular metabolism than bilayer structure. The most dramatic change we find in a single phospholipid species is the almost 24% (11.6 mol%) increase in 18:0-20:4 PI (Table 6). This PI species is a primary metabolite involved in signal transduction pathways through hydrolysis in the plasma membrane of its phosphorylated form (phosphatidylinositol 4,5-bisphosphate) to diacylglycerol and inositol 1,4,5-trisphosphate (IP_3). Release of IP_3 results in calcium mobilization from the endoplasmic reticulum in most cells [50]. In skeletal SR an IP_3-activated calcium channel has been reported [51], indicating the presence of this signalling pathway in skeletal muscle. Since cellular phospholipids are primarily synthesized on the cytoplasmic leaflet of the SR, the age-related changes we observe in this signal-specific PI species in SR membranes may reflect increased synthesis of a pool of phospholipids that are destined for export to the inner leaflet of the plasma membrane. Increased levels of synthesis of this species might represent an adaptive change to compensate for an age-dependent decreased capacity elsewhere in this signal transduction pathway. Alternatively, these changes may reflect less efficient transport of these species to the plasma membrane resulting in their accumulation in the SR.

Another striking result with respect to phospholipid composition of the SR is the substantial age-related increase in ethanolamine plasmalogens (Table 5). More than half of the ethanolamine glycerophospholipids in SR are plasmenylethanolamines, having a vinyl ether rather than an ester linkage at the *sn*-1 position. In contrast, choline plasmalogens are a minor component in skeletal SR [32]. The functional role of plasmalogens is not well-understood. These glycerophospholipids are found in high abundance in electrically active tissues, especially in brain and heart [52]. *sn*-2 substituents of plasmalogens are typically long chain polyunsaturated fatty acids. The frequent occurrence of arachidonic acid in plasmalogens has led to the suggestion that plasmalogens may represent a sequestered pool of arachidonic acid that can be released by plasmalogen-specific phospholipases for use in biosynthesis of eicosanoid metabolites [53]. Under ischemic conditions, plasmenylethanolamines in heart microsomes have been shown to be selectively degraded, presumably through the action of a plasmalogen-specific phospholipase whose activity is induced by ischemia [54]. Although these observations suggest an important role in both normal and pathological processes for plasmenylphospholipids, insufficient information is currently available to allow accurate inter-

pretation of the age-related changes in these species that we observe in skeletal muscle SR.

4.6. Relationship of work to aging studies

The free radical theory of aging suggests that aging is associated with an imbalance in which production of reactive oxygen species exceeds the protective ability of the cell. As a result the extent of oxidation of lipids, proteins, and nucleic acids is increased. It has been shown that the SR membrane with its substantial abundance of polyunsaturated acyl chains is highly susceptible to free radical attack [55]. However, the minimal degree of lysolipids that we observe in SR from aged animals indicates that the normally rapid turnover of lipids is efficient in aged organisms. Therefore the age-related shifts we observe in polyunsaturated chain species may indicate a remodelling of the metabolism of these free radical susceptible species (Tables 4–6). We note that a number of these changes, as well as those specifically involving PE plasmologens and the 18:0-20:4 PI species, are largely complete by middle-age, with little further changes occurring in senescence. This timecourse correlates with that observed for the production of oxygen free radicals in rat cardiac mitochondria [56]. If the observed timecourse represents a general phenomena in the other cell types, we might expect cellular responses, such as the changes we observe in skeletal SR, to follow a similar time-course. Nevertheless, whatever the specific alterations in lipid metabolism associated with aging, most importantly to the maintenance of calcium homeostasis, the cell maintains an overall lipid composition that provides for optimal bilayer fluidity and active calcium transport.

Acknowledgements

We wish to thank Mr. Robert Drake for acquisition of FAB spectra. The tandem mass spectrometer was purchased with the aid of a National Institutes of Health grant S10 RRO 6294-01 and the University of Kansas. This work was supported by grants from the Scientific Education Partnership, a Marion Merrell Dow Foundation and NIH GM46837. A.G.K. is a Postdoctoral Fellow of Marion Merrell Dow Foundation; on leave from the Biophysical Group, Institute of Chemical Kinetics and Combustion, Novosibirsk, 630090, Russia.

References

[1] Laganiere, S. and Fernandes, G. (1991) Lipids 26, 472–478.
[2] Söderberg, M., Edlung, C., Kristensson, K. and Dallner G. (1991) Lipids 26, 421–425.
[3] Guisto, N.M., Roque, M.E. and Ilincheta de Boschero, M.G. (1992) Lipids 27, 835–839.
[4] Vance, D.E. and Vance, J.E. (1985) Biochemistry of Lipids and Membranes, Benjamin/Cummings, Menlo Park.
[5] Houslay, M.D. and Stanley, K.K. (1982) in Dynamics of Biological Membranes, pp. 96–125, John Wiley and Sons, Chichester.
[6] Larsson, L. and Salviati, G. (1989) J. Physiol. 419, 253–264.
[7] Gafni, A. and Yuh, K. (1989) Mech. Ageing Dev. 49, 105–117.
[8] Ferrington, D.A., Jones, T.E., Squier, T.C. and Bigelow, D.J. (1993) Biophys. J. 64, A305.
[9] Wahnon, R., Mokady, S. and Cogan, U. (1989) Mech. Ageing Dev. 50, 249–255.
[10] Navarro, J., Toivio-Kunnikan, M. and Racker, E. (1984) Biochemistry 23, 130–135.
[11] Krainev, A.G., Bigelow, D.J. and Squier, T.C. (1993) Biophys. J. 64, A382.
[12] Fernandez, J.L., Rosemblatt, M. and Hidalgo, C. (1980) Biochim. Biophys. Acta 599, 552–568.
[13] Lanzetta, P.A., Alvarez, L.J., Reinach, P.S. and Candia, O.A. (1979) Anal. Biochem. 100, 95–97.
[14] Sabbadini, R.A. and Dahms, A.S. (1989) J. Bioenerg. Biomembr. 21, 163–213.
[15] Folch, J., Lees, M. and Sloane Stanley, G.H. (1957) J. Biol. Chem. 226, 497–509.
[16] Hidalgo, C., Ikemoto, N. and Gergely, J. (1976) J. Biol. Chem. 251, 4224–4232.
[17] Christie, W.W. (1987) in HPLC and Lipids, A Practical Guide, Pergamon Press, Oxford.
[18] Chen, P.S., Toribara, T.Y. and Warner, H. (1956) Anal. Chem. 28, 1756–1758.
[19] Allain, C.C., Poon, L.S., Chan, C.S.G., Richmond, W. and Fu, P.C. (1974) Clin. Chem. 20, 470–475.
[20] Blank, M.L. and Snyder, F. (1983) J. Chromatogr. 273, 415–420.
[21] Patton, G.M., Fasulo, J.M. and Robins, S.J. (1982) J. Lipid Res. 23, 190–196.
[22] Wiley, M.G., Przetakiewicz, M., Takahashi, M. and Lowenstein, J.M. (1992) Lipids 27, 295–301.
[23] Smith, M. and Jungalwala, F.B. (1981) J. Lipid Res. 22, 697–704.
[24] Blank, M.L., Robinson, M., Fitzgerald, V. and Snyder, F. (1984) J. Chromatogr. 298, 473–482.
[25] Gross, M.L., Jensen, N.J., Lippstren-Fisher, D.L. and Tomer, K.B. (1985) in Mass Spectrometry in the Health and Life Sciences (Burlingame, A.L. and Gastagnoli, N., Jr., eds.), pp. 209–238, Elsevier, Amsterdam.
[26] Squier, T.C. and Thomas, D.D. (1986) Biophys. J. 49, 937–942.
[27] Bigelow, D.J., Squier, T.C. and Thomas, D.D. (1986) Biochemistry 25, 194–202.
[28] Gaffney, B.J. (1976) in Spin Labeling (Berliner, L.J., ed.), pp. 576–671, Academic Press, New York.
[29] Gaffney, B.J. and Lin, D.C. (1976) in The Enzymes of Biological Membranes: Physical Chemical Techniques (Martonosi, A., ed.), Vol. I, pp. 71–90, Plenum Press, New York.
[30] Squier, T.C. and Thomas, D.D. (1986) Biophys. J. 49, 921–935.
[31] Jensen, N.J., Tomer, K.B. and Gross, M.L. (1987) Lipids 22, 480–491.
[32] Marai, L. and Kuksis, A. (1973) Can. J. Biochem. 51, 1365–1379.
[33] Hidalgo, C. (1985) Membrane Fluidity in Biology, Vol. 4, pp. 51–96, Academic Press, New York.
[34] Gennis, R.B. (1989) Biomembranes: Molecular Structure and Function, Springer-Verlag, Berlin.
[35] Yeagle, P.L. (1992) The Structure of Biological Membranes, CRC Press, Boca Raton.
[36] Bigelow, D.J. and Thomas, D.D. (1987) J. Biol. Chem. 262, 13449–13456.
[37] Squier, T.C., Bigelow, D.J. and Thomas, D.D. (1988) J. Biol. Chem. 263, 9178–9186.
[38] Birmachu, W. and Thomas, D.D. (1990) Biochemistry 29, 3904–3914.

[39] Thomas, D.D., Bigelow, D.J., Squier, T.C. and Hidalgo, C. (1982) Biophys. J. 37, 217–225.
[40] McConnel, H.M. and McFarland, B.G. (1972) Ann. N.Y. Acad. Sci. 195, 207–212.
[41] Squier, T.C. and Thomas, D.D. (1989) Biophys. J. 56, 735–748.
[42] Saffman, P.G. and Delbrück, M. (1975) Proc. Natl. Acad. Sci. USA 72, 3111–3113.
[43] Thomas, D.D. (1986) in Techniques for the Analysis of Membrane Proteins (Ragan, C.I. and Cherry, R.J., ed.), pp. 377–431, Chapman and Hall, London.
[44] Schneider, E.L. and Rowe, J.W. (1990) Handbook of the Biology of Aging, p. 81, 3rd Edn., Academic Press, New York.
[45] Rosemblatt, M., Hidalgo, C., Vergara, C. and Ikemoto, N. (1981) J. Biol. Chem. 256, 8140–8148.
[46] Fiehn, W., Peter, J.B., Mead, J.F. and Gan-Elepano, M. (1971) J. Biol. Chem. 246, 5617–5620.
[47] Kagawa, Y. (1974) Methods in Membrane Biology, Vol. I, Plenum Press, New York.
[48] Gurr, M.I. and Harwood, J.L. (1991) in Lipid Biochemistry, pp. 256–258, Chapman and Hall, London.
[49] Hidalgo, C., Thomas, D.D. and Ikemoto, N. (1978) J. Biol. Chem. 253, 6879–6887.
[50] Majerus, P.W., Wilson, D.B., Connolly, T.M., Bross, T.E. and Neufeld, E.J. (1986) Science 234, 1519–1526.
[51] Suarez-Isla, B.A., Irribarra, V., Oberhauser, A., Larralde, L., Bull, R., Hidalgo, C. and Jaimovich, E. (1988) Biophys. J. 54, 737–741.
[52] Scott, T.W., Setchell, B.P. and Bassett, J.M. (1967) Biochem. J. 104, 1040–1047.
[53] Gross, R.W. (1984) Biochemistry 23, 158–165.
[54] Hazen, S.L., Ford, D.A. and Gross, R.W. (1991) J. Biol. Chem. 266, 5629–5633.
[55] Kagan, V.E. (1988) Lipid Peroxidation in Biomembranes, CRC Press, Boca Raton.
[56] Guarnieri, C., Muscari, C. and Caldarera, C.M. (1992) in Free Radicals and Aging (Emerit, I. and Chance, B., eds.), pp. 73–77, Birkhäuser Verlag, Basel.